Automated detection and analysis of Ca^{2+} sparks in x-y image stacks using a novel algorithm implemented within the open-source image analysis platform, ImageJ

Elliot M. Steele and Derek S. Steele

School of Biomedical Sciences, University of Leeds, Leeds, England, LS29JT

Supplementary data

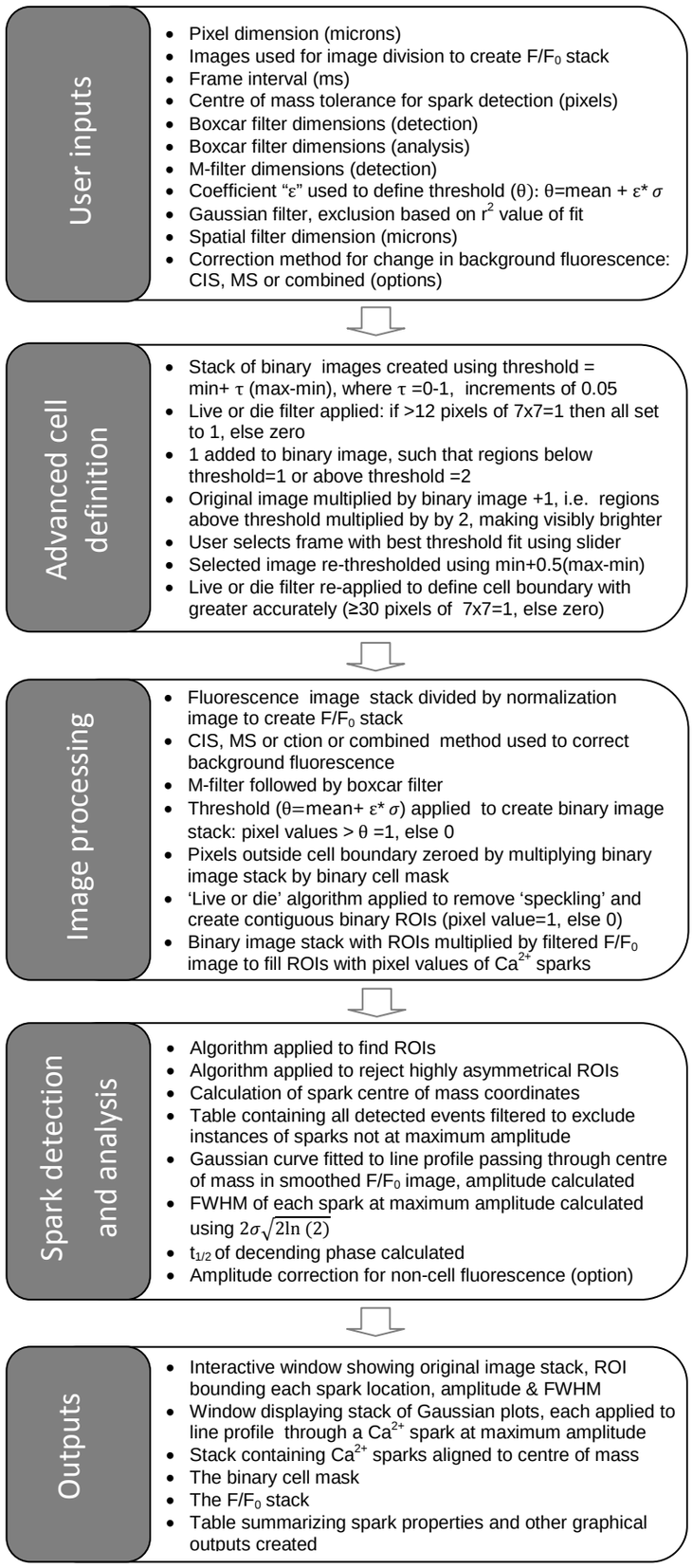

FIGURE S1: Summary of xySpark. The entry of user settings is followed by the advanced cell definition algorithm, image processing, spark detection and analysis and finally, creation of outputs and a user interface to facilitate examination of the data.

Summary of xySpark algorithm

Fig. S1 shows a detailed summary of the xySpark algorithm: The algorithm begins by allowing the user to enter information about the input data (frame interval, pixel size), filter characteristics for image processing and analysis, and the coefficient 'ε', which multiplied by the SD (σ), defines the threshold for spark detection. The user also identifies 2 frames lacking sparks to be used for creation of the normalized F/F_0 image stack used throughout analysis. Spark detection and analysis are treated as 2 separate processes, allowing different filter characteristics to be used

during spark detection and subsequent analysis steps. It is also possible to include criteria for exclusion of events larger than a specified FWHM (spatial filter) or based on the r^2 of a Gaussian curve fitted to a line profile passing through the centre of mass of each spark at its maximum amplitude. The initial inputs also include options for correction of small changes in baseline fluorescence (consecutive image subtraction, median subtraction, or a combined method).

To accurately define the region of the image occupied by the cell (advanced cell definition), a series of threshold values (followed by a live-or-die filter to make contiguous) is applied to the first image of the original data stack. The user then selects the threshold value that best defines the cell boundary based on visual assessment of images in which the region above threshold is multiplied by 2 (i.e. brighter). This modified image is then thresholded and a second live-or-die filter applied to more tightly define the cell boundary. The resulting 'binary cell mask' is used to eliminate regions outside the cell from all subsequent analysis.

Creation of the F/F_0 stack is followed by correction (if selected) of changes in background fluorescence and the application of detection filters. The threshold is then applied to this processed F/F_0 stack, followed by a live-or die filter to produce a stack of binary images with ROIs (pixel value=1) corresponding to regions above threshold.

During Spark detection and analysis, binary images with ROIs are used to identify corresponding regions in the F/F_0 image with a user selected output filter applied. The coordinates of the centre of mass are calculated for each event and maximum amplitude and FWHM calculated from the Gaussian fit to the line profile. The half time ($t_{1/2}$) of the spark descending phase is calculated using an exponential fit to the amplitudes of each spark as it appears in successive frames from the peak onwards.

The output is presented as a window showing the original image stack with each spark identified by a bounding box. In addition, the spark co-coordinates, amplitude, width, duration and frequency are provided as a table, which can be saved to disk. Other outputs include a stack containing all of the detected events, the binary cell mask, line profiles for all sparks with corresponding Gaussian curves and the F/F_0 image stack.

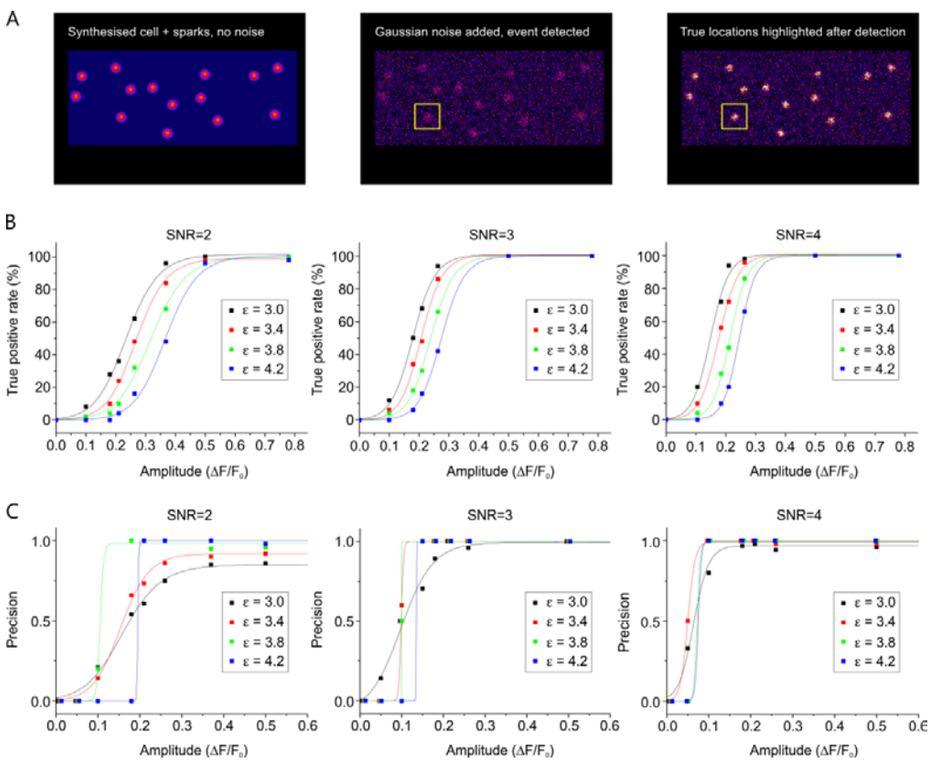

FIGURE S2 Characterisation of xySpark using synthetic images with sparks. (*A*) synthesised sparks, with a rectangle of raised fluorescence representing a cell (*left*), with added noise (*middle*) and after multipling the noise free image by the image with noise to highlight the sparks. ***(B)*** Percentage of known synthetic events of various amplitudes detected correctly as a function of amplitude ($\Delta F/F_0$) at SNR (mean background pixel value/σ) =2, 3 or 4 (*left, middle, right*), when mean background=38 and σ=19, 12.6 or 9.5. (*C)* Probability of event being correctly identified as a function of amplitude ($\Delta F/F_0$ = 0.05-0.78) and SNR = 2, 3 or 4 (*left, middle, right*). Each point=mean no. of events correctly identified/(mean no. events correctly identified + no. events wrongly identified).

To allow comparison with software for automatic detection and analysis of sparks in line-scan images, the performance of xySpark was evaluated using synthesised images containing a cell (mean cell background=38) and sparks of varying amplitudes, embedded in Gaussian noise (σ=19, 12.6 or 9.5) as a function of SNR and threshold (ε). Fig S2*A* shows a rectangular 'cell' with randomly located 'sparks', in the absence of noise (*left*). In this example, following addition of noise at σ=19 (*middle*), sparks were still detectable (box). However, at high noise and lower amplitudes it was sometimes difficult to identify the position of events and establish whether detection was correct or not. To address this, after analysis, the F/F_0 image was multiplied by an image that only contained the sparks (i.e. without cell or noise), thereby highlighting the position of each (*right*). Using this method, xySpark was used to define the number of true positive events detected (*B*) where $\Delta F/F_0$ varied between 0.05-0.78 and ε=3.0, 3.4, 3.8 or 4.2 at SNR=2 (*left*), 3 (*middle*) or 4 (*right*).

Both the sensitivity of detection and the shallowing of the relationships from SNR=2-4 is consistent with previously described algorithms used to detect sparks in line-scan images. Graphs showing the precision (events correctly detected/total events detected) at each SNR are also shown (*C*). At SNR=2, reducing ε from 3.4 to 3.0 shallows the relationship, due to an increased number of false positive events. The rapid transitions between 0 and 1 occur when the value of ε dictates that events below the threshold are excluded, but above the threshold, the sensitivity is such that all detected events are correctly identified. In practice, confocal images obtained from myocytes typically have an SNR ~4. At SNR=4 (*right*), setting ε = 3.4-3.8 results in relatively high sensitivity and precision, while at ε = 3.0, the shallower relationship peaking at <1 indicates the increased presence of false positives.

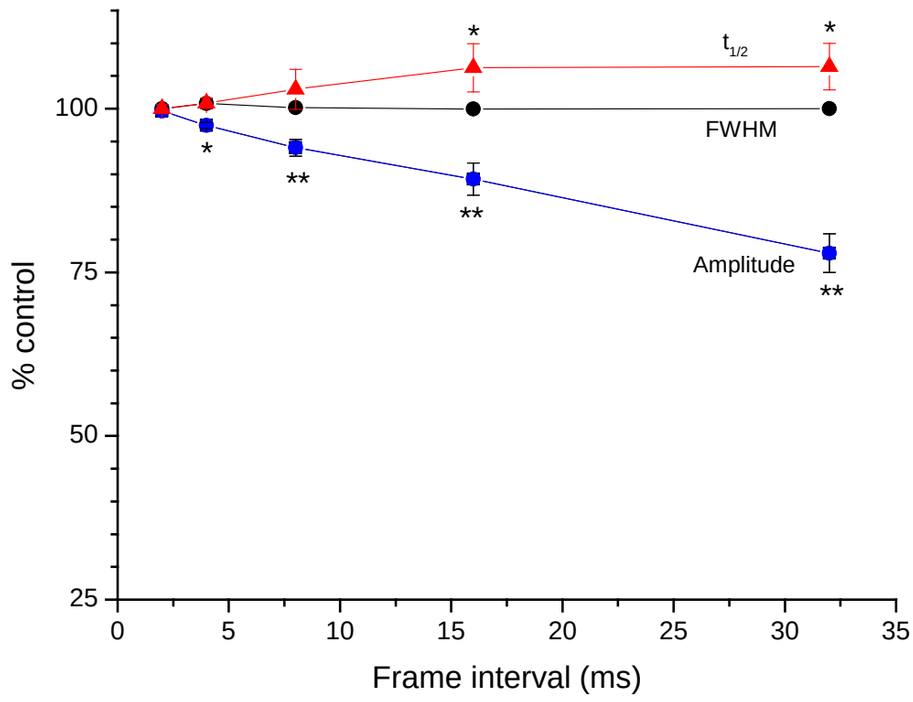

FIGURE S3. Detected spark amplitude, width and duration as a function of frame interval. Identical synthetic sparks were inserted at random time points into a stack, mimicking a recording at high temporal resolution. The "slice remover" function within ImageJ was then used to remove frames at set intervals, thereby simulating the effect of lower frame intervals of 2,4, 8, 16 or 32 ms. Each resulting stack was then analysed using xySpark to assess the effects of an increased frame interval (i.e. reduced sampling rate) on amplitude, duration and width. * $p<0.05$, **, $p<0.01$, n=50.

As shown in fig. S3, with increasing frame interval there was a progressive underestimation of spark amplitude ($\Delta F/F_0$) by 22.1 ± 2.9% (n=50) at the maximum frame interval tested (32 ms). There was no significant effect on mean width, while measured duration ($t_{1/2}$) increased slightly (by 6.4 ± 2.9 %, n=50) at a frame interval of 32 ms.